

## Supporting Information

# A New Water Oxidation Catalyst: Lithium Manganese Pyrophosphate with Tunable Mn Valency

Jimin Park,<sup>†, ||</sup> Hyunah Kim,<sup>†, ||</sup> Kyoungsuk Jin,<sup>†</sup> Byung Ju Lee,<sup>†</sup> Yong-Sun Park,<sup>†</sup> Hyungsub Kim,<sup>†</sup> Inchul Park,<sup>†</sup> Ki Dong Yang,<sup>†</sup> Hui-Yun Jeong,<sup>†</sup> Jongsoon Kim,<sup>†</sup> Koo Tak Hong,<sup>†, ‡</sup> Ho Won Jang,<sup>†, ‡</sup> Kisuk Kang,<sup>\*, †, ‡, §</sup> and Ki Tae Nam<sup>\*, †, ‡</sup>

<sup>†</sup>Department of Materials Science and Engineering, <sup>‡</sup>Research Institute of Advanced Materials (RIAM), and <sup>§</sup>Center for Nanoparticle Research, Institute for Basic Science (IBS), Seoul National University, 1 Gwanak-ro, Gwanak-gu, Seoul 151-742, Republic of Korea

\*To whom correspondence should be addressed.

E-mail: [matlgen1@snu.ac.kr](mailto:matlgen1@snu.ac.kr), [nkitae@snu.ac.kr](mailto:nkitae@snu.ac.kr)

## Synthesis of nanoparticles

$\text{Li}_2\text{MnP}_2\text{O}_7$  samples were prepared using conventional solid-state synthesis using stoichiometric mixture of  $\text{Li}_2\text{CO}_3$  (ACS reagent,  $\geq 99\%$ , Aldrich),  $\text{MnC}_2\text{O}_4 \cdot 2\text{H}_2\text{O}$  ( $\geq 99\%$ , Alfa Aesar), and  $(\text{NH}_4)_2\text{HPO}_4$  (ACS reagent 98%, Aldrich). These precursors were mixed by ball milling for 12 h. The precursor mixture was initially heated at 300 °C for 6 h under steady Ar flow. The calcined sample was pelletized using a disk-shaped mold, and calcined again at 600 °C for 10 h under steady Ar flow.

To prepare  $\text{Li}_{2-x}\text{MnP}_2\text{O}_7$ ,  $\text{Li}_2\text{MnP}_2\text{O}_7$  was chemically delithiated using  $\text{NO}_2\text{BF}_4$  (Aldrich, 95%) in acetonitrile solvents (99%, Aldrich) according to the following reaction



$\text{NO}_2\text{BF}_4$  was used as a strong oxidizing agent with a redox potential for  $\text{NO}_2^+/\text{NO}_2$  of 5.1 V versus  $\text{Li}^+/\text{Li}$ . The final product,  $\text{Li}_{2-x}\text{MnP}_2\text{O}_7$ , was obtained by washing the reactants several times with acetonitrile.

## Characterization of nanoparticles

### A. Crystal Structure analysis : Powder X-ray diffraction and Rietveld refinement

Powder X-ray diffraction (XRD) was performed on a D-8 Advance X-ray diffractometer with Cu  $K\alpha$  radiation ( $\lambda=1.54056 \text{ \AA}$ ). XRD patterns were recorded in a range of 10-80° with a step size of 0.01°. The resulting XRD patterns were compared with previously reported one.<sup>1</sup>

Rietveld refinement was performed using TOPAS Academic. The crystal structure of  $\text{Li}_{2-x}\text{MnP}_2\text{O}_7$  was drawn with VESTA program based on its atomic coordination information. The maximum bond length between manganese atom and oxygen atom was set to 2.6 Å.

### **B. Transmission electron microscopy (TEM) Analysis**

TEM images and selected area electron diffraction (SAED) patterns were obtained using a high resolution transmission electron microscope (JEM-3000F, JEOL, Japan) with an acceleration voltage of 300 kV. The TEM samples were collected from as-prepared compounds or from FTO glass directly following the electrochemical measurement and were dispersed in ethanol by sonication for approximately 5 min. Approximately 10  $\mu\text{l}$  of dispersed  $\text{Li}_{2-x}\text{MnP}_2\text{O}_7$  was dropped on the lacy carbon TEM grid and air-dried and then further dried in a vacuum oven at 70 °C for 30 min to evaporate the solvent.

### **C. Elemental analysis**

Inductively coupled plasma-mass spectrometer (ICP/MS, 720-ES, Varian) measurements were conducted to determine the exact chemical composition of the  $\text{Li}_{2-x}\text{MnP}_2\text{O}_7$  ( $x=0, 0.3, 0.5, 1$ ) nanoparticles.

### **D. BET analysis**

Brunauer-Emmett-Teller (BET) analysis was conducted on the  $\text{Li}_{2-x}\text{MnP}_2\text{O}_7$  ( $x=0, 0.3, 0.5, 1$ ) compounds, MnO, and MnO<sub>2</sub>. In total, 0.5070 g of the sample was loaded in the BET analyzer (Physisorption Analyzer, Micromeritics, USA) under an N<sub>2</sub> adsorption environment.

## **E. XPS analysis**

X-ray photo-electron spectroscopy (XPS) spectra were obtained by electron spectroscopy (Sigma Probe; Thermo VG Scientific, UK) with a pass energy of 30 eV and a step size of 0.1 eV. All the binding energies are referenced to C 1s (284.5 eV).

## **F. XAS analysis**

The valence states of Manganese in  $\text{Li}_{2-x}\text{MnP}_2\text{O}_7$  ( $x = 0, 0.3, 0.5, 1$ ) samples were investigated by X-ray absorption near-edge structure (XANES) analysis. The XAS experiments were performed at room temperature at beamline 1D and 8C at the Pohang Accelerator Laboratory (PAL), Republic of Korea. They were collected in the fluorescence mode at the manganese K-edge XANES spectra using electron energy of 2.5 GeV and a current of 250mA top-up mode. Mn K-edge energy calibration was performed using Mn metal foil as a reference.

# **Electrochemical measurements**

## **A. Electrochemical Methods**

All the electrochemical experiments were conducted in a three-electrode electrochemical cell system. A BASi Ag/AgCl/3M NaCl reference electrode and Pt foil (2 cm × 2 cm × 0.1 mm, 99.997% purity, Alfa Aesar) were used as the reference electrode and counter electrode, respectively. The electrochemical tests were performed at ambient temperature ( $21 \pm 1^\circ\text{C}$ ) using a potentiostat system (CHI 760C, CH Instruments, Inc.). The electrode potential was converted to the NHE scale using the following equation:  $E(\text{NHE}) = E(\text{Ag}/\text{AgCl}) + 0.197 \text{ V}$ . Additionally,

the overpotential values were calculated from the difference between the  $iR$  corrected potential ( $V = V_{\text{applied}} - iR$ ) and the thermodynamic point of water oxidation at a specified pH. The electrolyte was a phosphate buffer with a designed buffer strength under pH 7.0. The electrolyte was degassed by bubbling with high-purity nitrogen (99.999%) for at least 1 hour before the start of each experiment.

## **B. Cyclic Voltammetry**

The preparation procedure of the working electrodes containing our catalysts can be described as follows. First, 5 mg of the catalyst powder was dispersed in 1 ml of deionized water mixed with 100  $\mu\text{l}$  of neutralized Nafion solution. Then, the mixture was sonicated for at least 30 min to produce homogeneous ink. Next, 50  $\mu\text{l}$  of the catalyst solution was dropped onto the FTO substrate, and spin-coating was performed at 2000 rpm for 30 sec. Finally, the prepared working electrode was dried in an 80 °C oven for 5 min before the CV measurements. The weight of the catalyst onto the FTO substrate was carefully measured by a micro weighing electronic scale (Sartorius Micro Balance). Before every electrochemical experiment, the solution resistance was measured in the electrolysis bath. All the data were  $iR$ - compensated. For the stability test, the working electrode was cycled 100 times, with the potential range from 0.7 V to 1.5 V versus NHE at a scan rate of 10 mV/sec.

## **C. Galvanostatic Charging-Discharging measurement**

Electrodes were fabricated using the active material  $\text{Li}_2\text{MnP}_2\text{O}_7$ , super P and polyvinylidene fluoride (PVDF) at a weight ratio of 70:20:10 in N-methyl-2-pyrrolidone (NMP) (99.5%, Aldrich) solvent. The mixed slurry was pasted onto Al foil using a doctor blade method,

and the NMP was allowed to evaporate at 120 °C for 3 h. The Li-ion cell was assembled in a CR2032-type coin cell in an Ar-filled glovebox using a lithium metal foil as a negative electrode, Celgard separator and 1 M solution of LiPF<sub>6</sub> in a mixture of ethyl carbonate/dimethyl carbonate (EC/DMC, 1:1 v/v) as an electrolyte. Galvanostatic charge/discharge measurements were conducted at a C/20. The C-rate is based on the theoretical capacity of 110 mAh g<sup>-1</sup>, which corresponds to 1 Li extraction/insertion of Li<sub>2</sub>MnP<sub>2</sub>O<sub>7</sub>.

## Computational Study

The first principles calculations were conducted to determine the energies of given structures, based on spin-polarized generalized gradient approximation (GGA) using Perdew-Burke-Ernzerhof (PBE) exchange-correlation parameterization and density functional theory (DFT). We applied the Hubbard parameter (GGA+U) to correct the incomplete cancelation of the self-interaction of GGA. Ab initio quantum mechanical calculation was performed with the Vienna ab initio simulation package (VASP) using the projector-augmented wave (PAW) method. A plane-wave basis with an energy cutoff was 500 eV and appropriate k-point meshes were sampled by a 2×2×2 monkhorst-pack mesh. All structures are fully relaxed. The atomic charges were calculated by the Voronoi spin integration.

**Table S1** Inductively coupled plasma - mass spectrometer (ICP/MS) data for the  $\text{Li}_{2-x}\text{MnP}_2\text{O}_7$  ( $x = 0, 0.3, 0.5, 1$ ) powders before and after bulk-electrolysis at the potential of 1.5 V vs NHE for 3 h. After the OER, the ratio of Li ions to Mn ions was maintained in each sample.

Li/Mn ratio	Raw Sample	Bulk electrolyzed Sample ( 1.5 V vs NHE for 3 h)
$\text{Li}_2\text{MnP}_2\text{O}_7$	2.017	1.991
$\text{Li}_{1.7}\text{MnP}_2\text{O}_7$	1.686	1.704
$\text{Li}_{1.5}\text{MnP}_2\text{O}_7$	1.523	1.546
$\text{LiMnP}_2\text{O}_7$	1.002	0.996

**Table S2.** Simulated lattice parameters and unit cell volume of  $\text{Li}_{2-x}\text{MnP}_2\text{O}_7$ .

Designation	$a$ (Å)	$b$ (Å)	$c$ (Å)	$\beta$ (deg)	Vol (Å <sup>3</sup> )
$\text{Li}_2\text{MnP}_2\text{O}_7$	9.916	9.829	11.180	102.467	1063.930
$\text{Li}_{1.75}\text{MnP}_2\text{O}_7$	9.909	9.894	11.282	102.283	1080.859
$\text{Li}_{1.5}\text{MnP}_2\text{O}_7$	9.916	9.850	11.223	101.833	1072.864
$\text{LiMnP}_2\text{O}_7$	9.978	9.666	11.085	99.868	1053.371

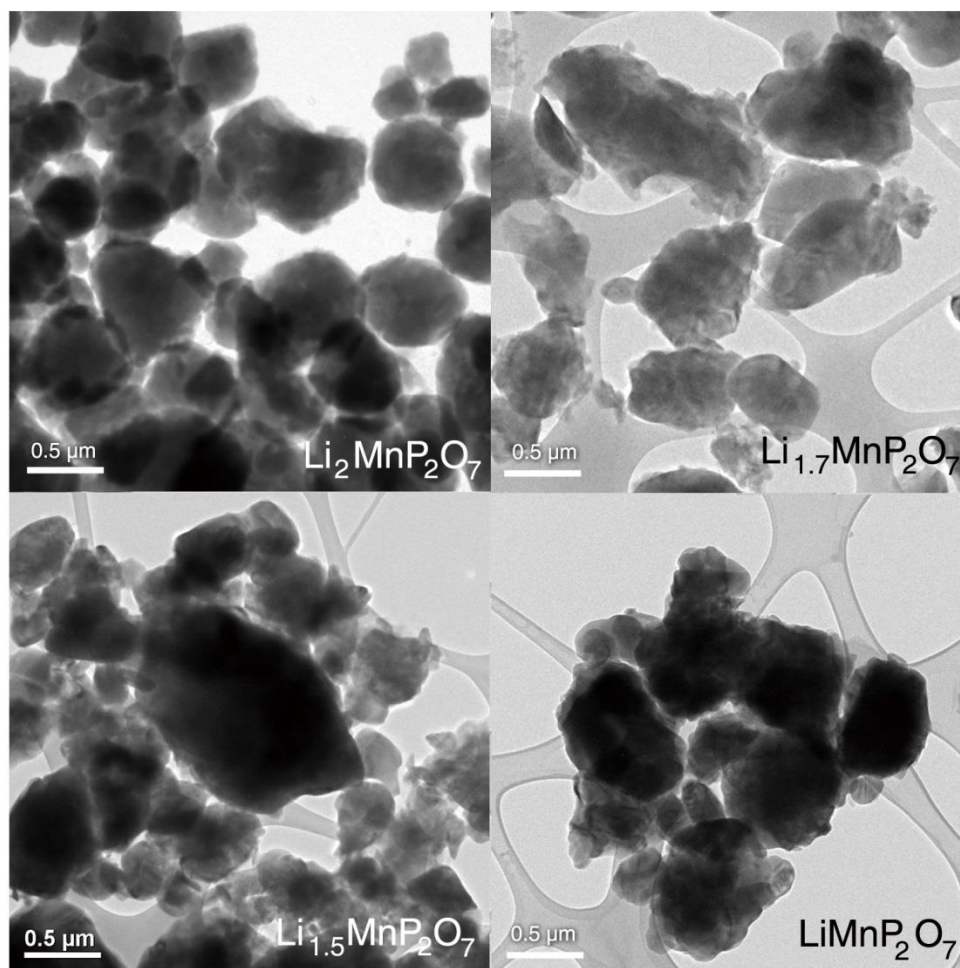


**Figure S1.** TEM images for  $\text{Li}_2\text{MnP}_2\text{O}_7$ ,  $\text{Li}_{1.7}\text{MnP}_2\text{O}_7$ ,  $\text{Li}_{1.5}\text{MnP}_2\text{O}_7$ , and  $\text{LiMnP}_2\text{O}_7$ . There is no significant difference in morphology, size of the particles. The surface areas of the compounds were obtained based on five independent BET measurements. ( $\text{Li}_2\text{MnP}_2\text{O}_7$ :  $1.024 \pm 0.06 \text{ m}^2/\text{g}$ ,  $\text{Li}_{1.7}\text{MnP}_2\text{O}_7$ :  $1.055 \pm 0.04 \text{ m}^2/\text{g}$ ,  $\text{Li}_{1.5}\text{MnP}_2\text{O}_7$ :  $1.094 \pm 0.11 \text{ m}^2/\text{g}$ ,  $\text{Li}_2\text{MnP}_2\text{O}_7$ :  $1.131 \pm 0.07 \text{ m}^2/\text{g}$ )

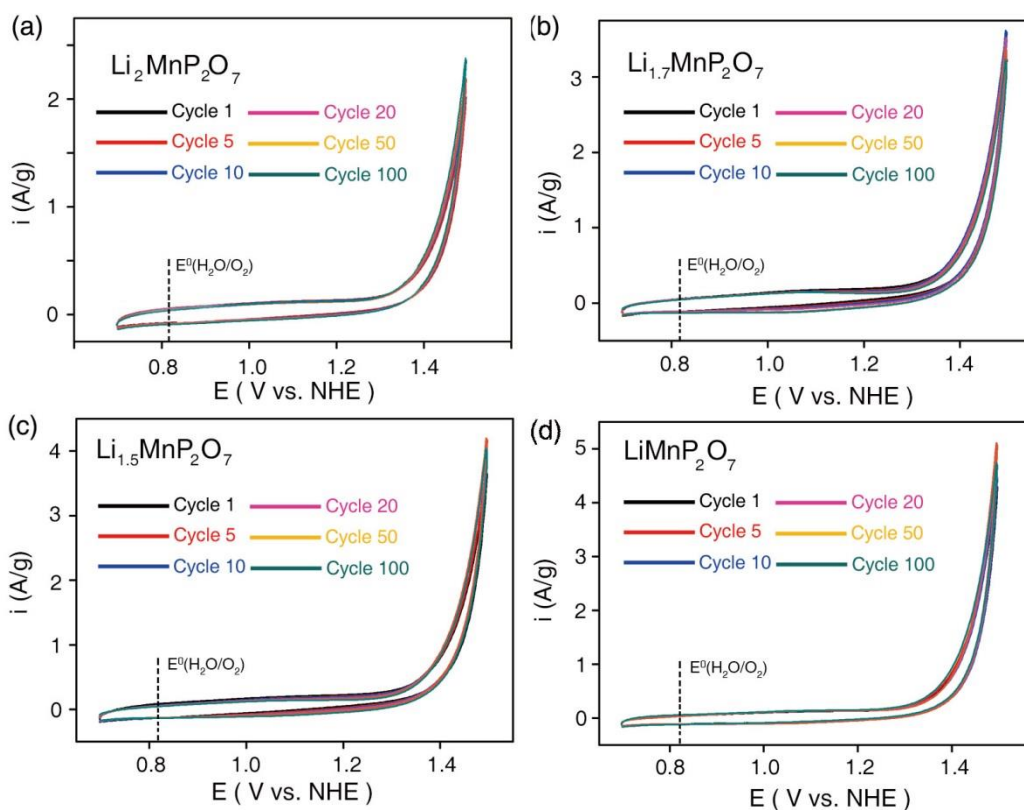


**Figure S2.** Cyclic voltammetry curves of  $\text{Li}_2\text{MnP}_2\text{O}_7$  (a),  $\text{Li}_{1.7}\text{MnP}_2\text{O}_7$  (b),  $\text{Li}_{1.5}\text{MnP}_2\text{O}_7$  (c) and  $\text{LiMnP}_2\text{O}_7$  (d) before polarization correction. All the cyclic voltammetry curves were obtained in  $\text{N}_2$ -saturated 0.5 M sodium phosphate buffer (pH 7.0) at a scan rate of 10 mV/sec. Even after 100 cycles of voltammetry cycling, the OER currents and pseudocapacitive currents almost remained constant. The thermodynamic potential for water oxidation is marked at 0.816 V vs. NHE (pH 7).

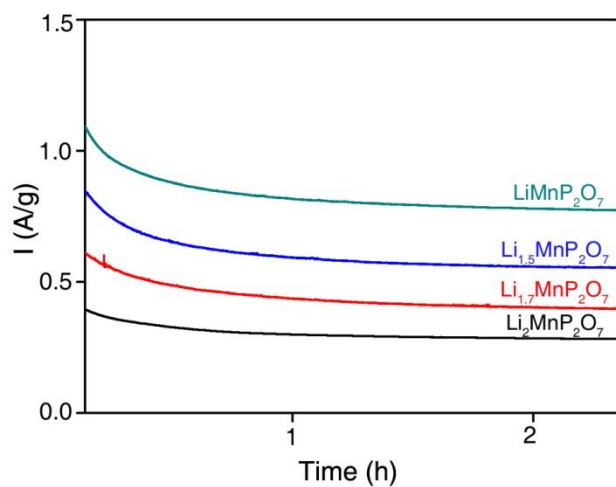


**Figure S3.** Catalytic current profile of  $\text{Li}_{2-x}\text{MnP}_2\text{O}_7$  ( $x = 0, 0.3, 0.5, 1$ ) obtained under constant potential (1.4 V vs. NHE) electrolysis at pH 7.0. The saturated value is almost the same as the averaged current shown in Figures 3a.

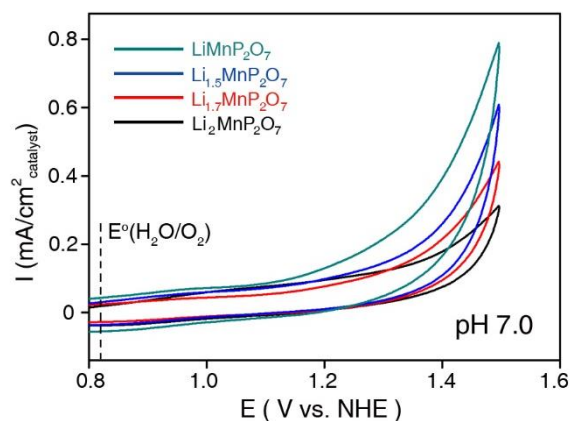


**Figure S4.** Cyclic voltammetry curves of  $\text{LiMnP}_2\text{O}_7$  (green),  $\text{Li}_{1.5}\text{MnP}_2\text{O}_7$  (blue),  $\text{Li}_{1.7}\text{MnP}_2\text{O}_7$  (red) and  $\text{Li}_2\text{MnP}_2\text{O}_7$  (black) electrodes in 0.5 M sodium phosphate buffer (pH 7.0) at a scan rate of 10 mV/sec at 900 rpm. All the working electrodes were prepared with a final loading of 0.25  $\text{mg}_{\text{catalyst}}/\text{cm}^2_{\text{disk}}$ , 0.05  $\text{mg}_{\text{carbon}}/\text{cm}^2_{\text{disk}}$ , and 0.05  $\text{mg}_{\text{Nafion}}/\text{cm}^2_{\text{disk}}$ .

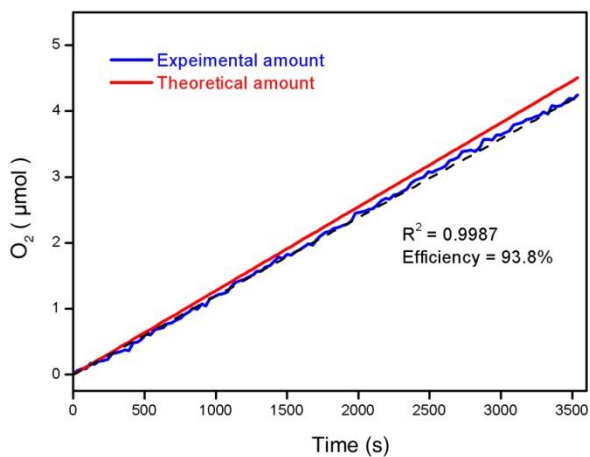


**Figure S5.** The amount of evolved O<sub>2</sub> molecules measured by fluorescent sensor (blue line) and the theoretical amount of evolved O<sub>2</sub> (red line) during the bulk electrolysis at the applied potential of 1.5 V vs. NHE for 1 h. Before the bulk electrolysis at the applied potential of 1.5 V vs. NHE, the electrolyte was degassed by bubbling with high purity N<sub>2</sub> for 3 h. The theoretical amount of O<sub>2</sub> molecules was calculated, assuming a Faradaic efficiency of 100%. The trend line of the measured O<sub>2</sub> molecules was indicated in dashed black line ( $R^2=0.9987$ ).

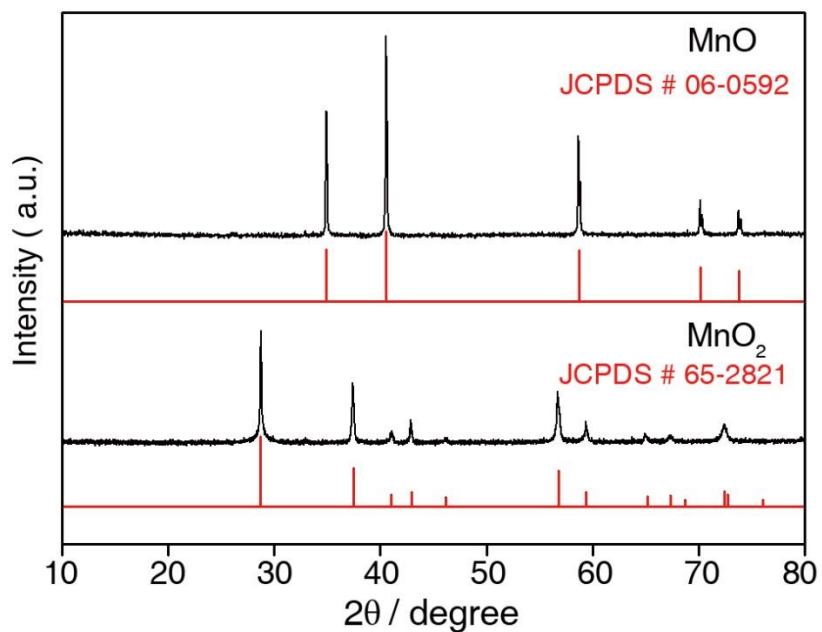


**Figure S6.** X-ray diffraction patterns of commercial MnO, MnO<sub>2</sub> powder (black). The patterns are consistent with those previously reported (red). (MnO : JCPDS # 06-0592, MnO<sub>2</sub> JCPDS # 65-2821) XRD pattern shows that each material has monophasic features and there are no secondary phases.

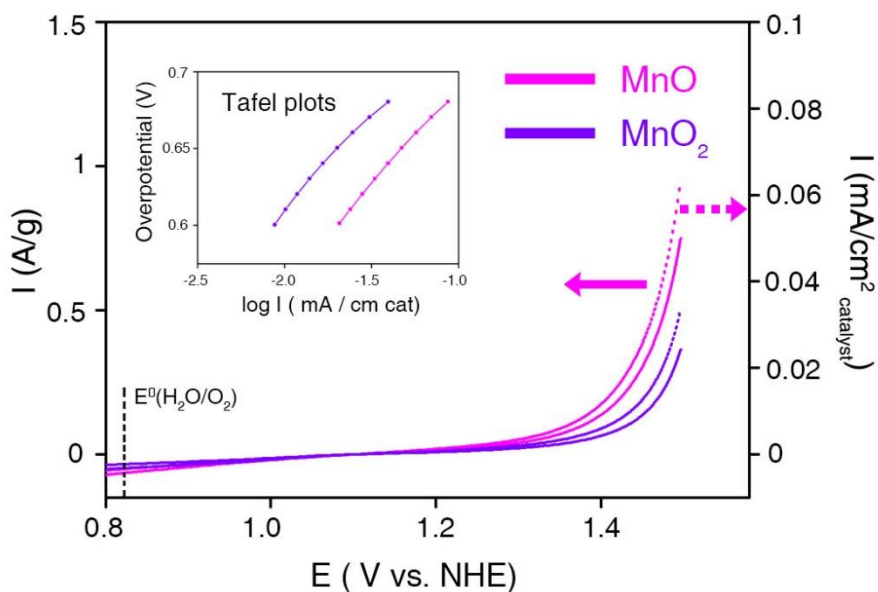


**Figure S7.** Polarization-corrected cyclic voltammetry curves and their Tafel plots normalized to the surface area of the catalyst (inset) for MnO, MnO<sub>2</sub>. The polarization-corrected curves were obtained by averaging the currents of the forward and reverse CV scans. The current value was normalized to the total weight (solid line) and the total surface area of the catalyst (dashed line), respectively. The thermodynamic potential for water oxidation is marked at 0.816 V vs. NHE (pH 7). To obtain the Tafel plot, all the samples were normalized to the initial surface area of the particles on the working electrode. Particle surface area was obtained by BET analysis. (MnO : 1.18 m<sup>2</sup>/g , MnO<sub>2</sub> : 1.08 m<sup>2</sup>/g ).

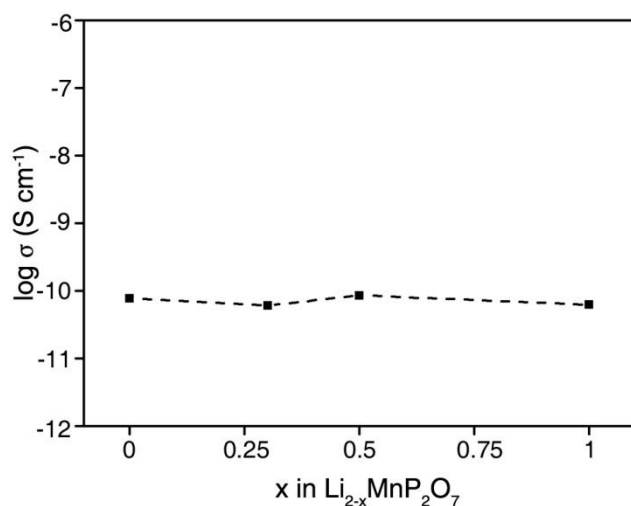


**Figure S8.** The change in electron conductivity of the pellets as a function of Li content in Li<sub>2-x</sub>MnP<sub>2</sub>O<sub>7</sub> (x=0.0-1.0). Electron conductivity was measured using four-point van der Pauw methods.<sup>2</sup> The catalysts were pressed into pellets with 15 mm diameters and ~2 mm thicknesses using a uniaxial press (400 kg cm<sup>-2</sup>). They were further compacted at 200 MPa for 10 min using cold isostatic pressing. A compactness of ~ 85% of the pellet was obtained without sintering. The 75-nm-thick platinum patterns were deposited on top sides of the pellets by sputtering using a Cr mask to ensure ohmic contacts. The sheet resistances of the pellets were measured using the van der Pauw method<sup>1</sup> with an Agilent 4156 C precision semiconductor parameter analyzer. The conductivities of the pellets were calculated using the following equation:

$$\sigma = \frac{1}{\rho} = \frac{1}{R_s \times t}$$

where  $\sigma$ ,  $R_s$  and  $t$  are the conductivity, sheet resistance and thickness of the pellets, respectively. All the pellets showed almost similar conductivity values.

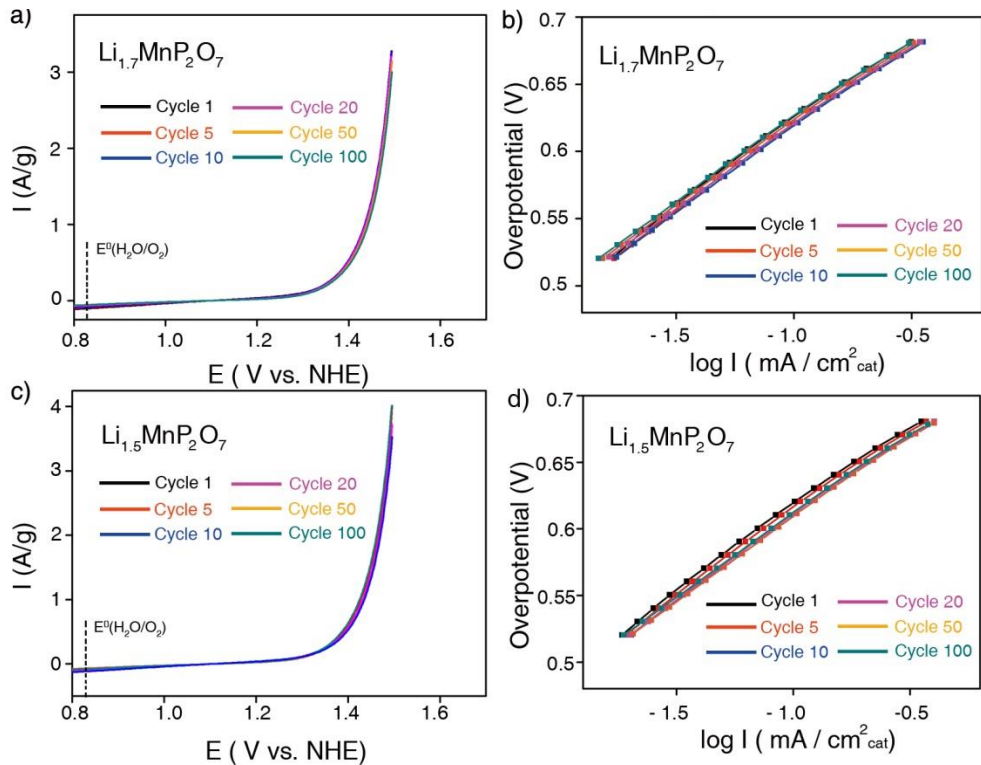


**Figure S9.** Polarization-corrected cyclic voltammetry curves of  $\text{Li}_{1.7}\text{MnP}_2\text{O}_7$  (a) and  $\text{Li}_{1.5}\text{MnP}_2\text{O}_7$  (c) showing the 1<sup>st</sup>, 5<sup>th</sup>, 10<sup>th</sup>, 20<sup>th</sup>, 50<sup>th</sup> and 100<sup>th</sup> cycles. The polarization-corrected curves were obtained by averaging the currents of the forward and reverse CV scans. All the cyclic voltammetry curves were obtained in an  $\text{N}_2$ -saturated 0.5 M sodium phosphate buffer (pH 7.0) at a scan rate of 10 mV/sec. Tafel plots of the cycled data for selected cycles of  $\text{Li}_{1.7}\text{MnP}_2\text{O}_7$  (b) and  $\text{Li}_{1.5}\text{MnP}_2\text{O}_7$  (d). The thermodynamic potential for water oxidation is marked at 0.816 V vs. NHE (pH 7).

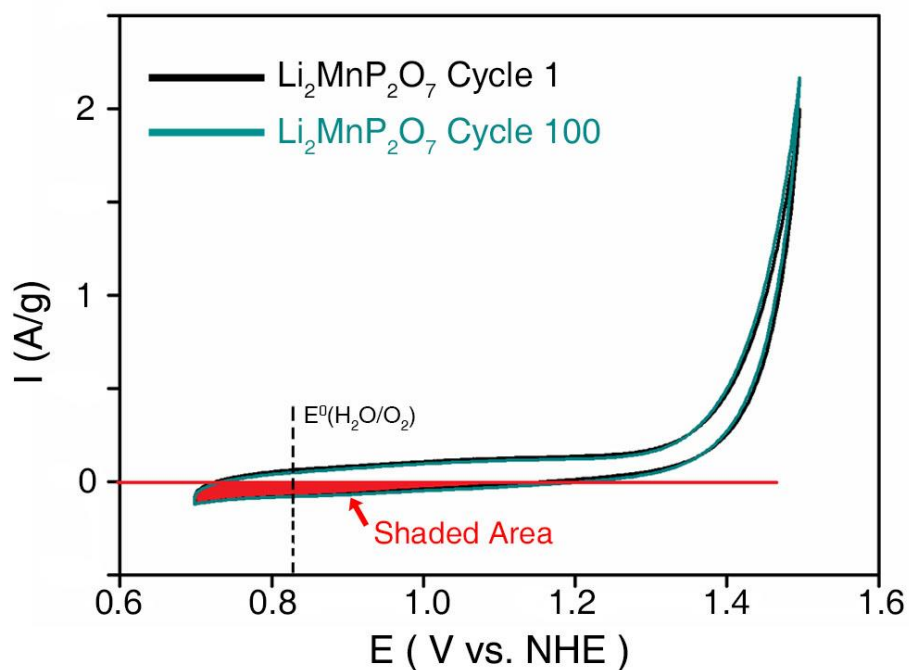


**Figure S10.** Cyclic voltammetry curves of  $\text{Li}_2\text{MnP}_2\text{O}_7$  showing the 1<sup>st</sup> and 100<sup>th</sup> cycles; the current was normalized to the weight of the catalyst on the FTO substrate. The shaded area during the negative-going scan can be proportional to the cathodic charge. The cathodic charge is proportional to the pseudocapacitance and the surface area of the catalysts onto the FTO substrate. The shaded areas of the two curves are almost identical, indicating that the surface area of  $\text{Li}_2\text{MnP}_2\text{O}_7$  remains nearly constant during the OER. The thermodynamic potential for water oxidation is marked at 0.816 V vs. NHE (pH 7).

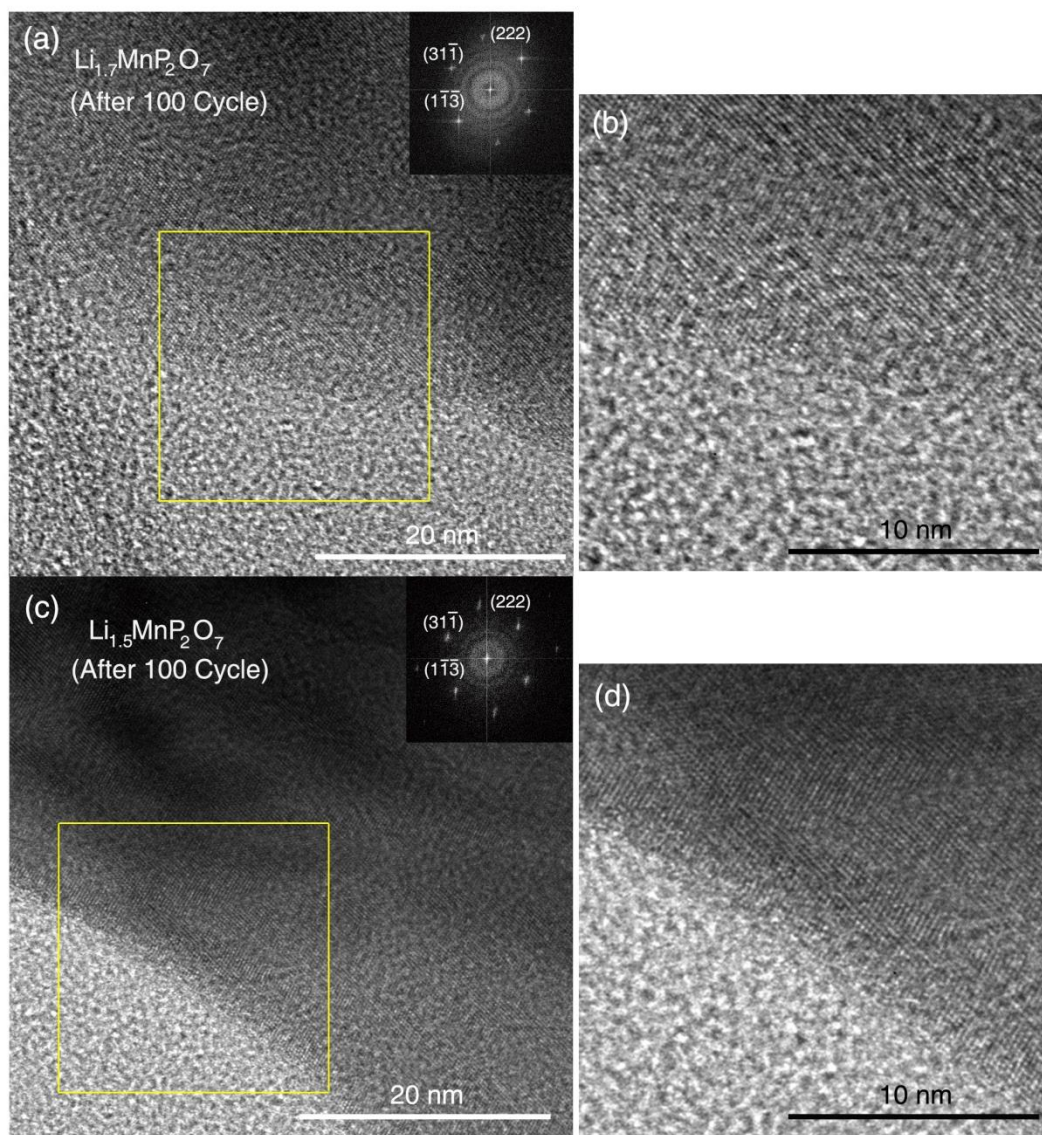


**Figure S11.** HRTEM images (left) and FFTs (inset) of the interface regions of  $\text{Li}_{1.7}\text{MnP}_2\text{O}_7$  (a) and  $\text{Li}_{1.5}\text{MnP}_2\text{O}_7$  (c) after 100 continuous cycles at a scan rate of 10 mV/s from 0.7 V to 1.5 V vs. NHE in 0.5 M sodium phosphate buffer at pH 7. (b) and (d) are high magnitude images of selected areas (yellow squares) of (a) and (b), respectively. HRTEM images for  $\text{Li}_{1.7}\text{MnP}_2\text{O}_7$  and  $\text{Li}_{1.5}\text{MnP}_2\text{O}_7$  also revealed high crystallinity even after 100 cycles from 0.7 V to 1.5 V versus NHE.

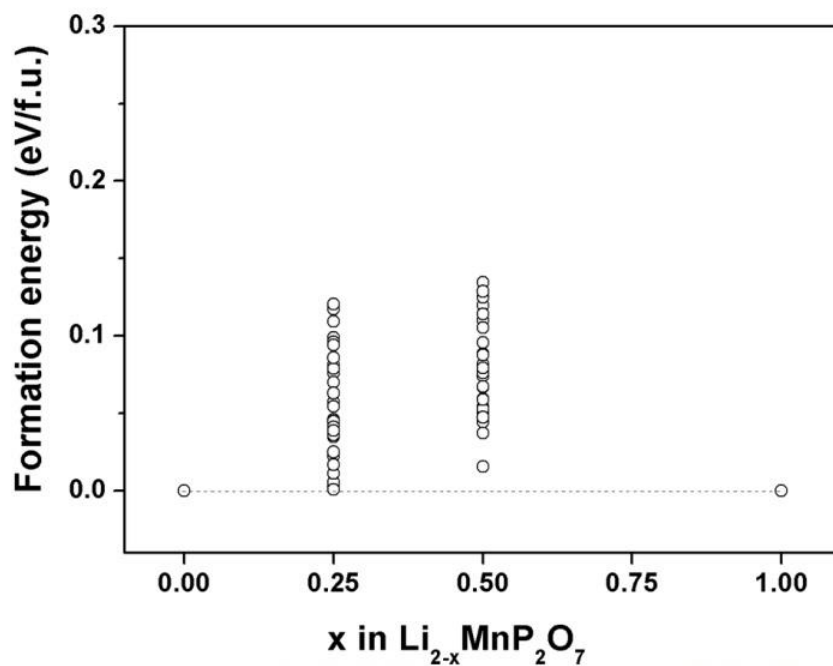


**Figure S12.** Calculated formation energies at various compositions ( $x = 0, 0.25, 0.5, 1$ ) and a convex hull of  $\text{Li}_{2-x}\text{MnP}_2\text{O}_7$ . A series of possible crystal structures of  $\text{Li}_{2-x}\text{MnP}_2\text{O}_7$  ( $x = 0.25, 0.5, 1$ ) and their relative energies were identified (blank circle). We selected the most stable structures in each composition ( $x = 0.25, 0.5, 1$ ) as the theoretical models of  $\text{Li}_{1.75}\text{MnP}_2\text{O}_7$ ,  $\text{Li}_{1.5}\text{MnP}_2\text{O}_7$ , and  $\text{LiMnP}_2\text{O}_7$  structures.

## Reference

(1) Tamaru, M.; Barpanda, P.; Yamada, Y.; Nishimura, S.-i.; Yamada, A. *J. Mater. Chem.* **2012**, *22*, 24526.

(2) Van der Pauw, L. *Philips Tech. Rev.* **1958**, *20*, 220.